

## Film cooling with using the decomposition of an $\text{NH}_3$ cooling stream as a chemical heat sink

CHENG KeYong<sup>1,2</sup>, CHEN Wei<sup>1,2</sup>, LIANG ShiQiang<sup>1\*</sup>, GUO YongXian<sup>1</sup>, HUAI XiuLan<sup>1</sup> & GUI XiaoHong<sup>1</sup>

<sup>1</sup> Institute of Engineering Thermophysics, Chinese Academy of Sciences, Beijing 100190, China;

<sup>2</sup> Graduate University of Chinese Academy of Sciences, Beijing 100049, China

Received October 17, 2011; accepted March 23, 2012

The inlet temperatures of gas turbines are generally increasing over time, so conventional cooling methods are likely to approach their useful limits. It is therefore essential to investigate novel cooling methods. Based on the theory of heat transfer enhancement, a novel film cooling method for gas turbine blades using a chemical heat sink is proposed. In this method, the endothermic reaction of an  $\text{NH}_3$  cooling stream heated by the main gas stream takes place, reducing the convective heat transfer between the main-stream and the blades. Therefore, film cooling effectiveness is improved. To test the feasibility of the proposed method, numerical simulations were conducted, using the classical flat plate with a 30 degree angled cylindrical hole (diameter,  $D$ ). Film cooling effectiveness at different blowing ratios ( $M = 0.5, 1.0, \text{ and } 1.5$ ) were computed and compared with the results of conventional cooling methods. The simulation results show that the proposed method can enhance film cooling effectiveness not only in the stream-wise direction, but also in the span-wise direction. The span-averaged film effectiveness is improved in the presence of a chemical heat sink, with the value of  $X/D$  (the ratio of downstream distance from the center of the film hole to the diameter of the film hole) increasing downstream of the film hole. The novel film cooling approach showed the best performance at  $M = 0.5$ .

**reaction, heat sink, film cooling, heat transfer, numerical simulation**

**Citation:** Cheng K Y, Chen W, Liang S Q, et al. Film cooling with using the decomposition of an  $\text{NH}_3$  cooling stream as a chemical heat sink. *Chin Sci Bull*, 2012, 57: 3652–3659, doi: 10.1007/s11434-012-5304-y

Modern gas turbine engines are typically operated with high inlet temperatures, which are far beyond the melting points of metal components. This requirement necessitates the design of highly efficient cooling techniques. In the past few decades, film cooling technology has played a major role in the advancement of gas turbines to higher firing temperatures and longer life parts. Many investigations have been performed by a broad spectrum of researchers to understand the fundamental physics of film cooling. The primary focus of most research has been on the use of discrete film holes. Cylindrical holes are widely used because of their ease of manufacture. Kercher [1] presented an exhaustive list of film cooling literature that focused on cylindrical holes. However, this type of cooling structure

clearly shows jet lift-off behavior and therefore, many methods are used to remedy this problem. Bunker [2] provided an excellent overview of the literature involving shaped film cooling holes and examined the origins of shaped film cooling, summarizing the extant knowledge concerning the performance of such film cooling holes. It was confirmed that cooling effectiveness of shaped holes is better than that of the cylindrical holes. However, they are limited by technical difficulties during manufacture. Therefore, Heidmann et al. [3–5] again considered cylindrical holes and studied an anti-vortex arrangement in which one primary cooling hole is accompanied by two small side holes. Detailed flow visualization showed that as expected, the design counteracted the detrimental vorticity of the cylindrical hole flow, allowing it to remain attaching to the surface. Compared with the standard cylindrical hole, an improvement in

\*Corresponding author (email: [liangsq@mail.etp.ac.cn](mailto:liangsq@mail.etp.ac.cn))

film effectiveness of about 0.2 was demonstrated. At the same time, many other film cooling designs have been proposed over the years to improve film cooling effectiveness. Graf et al. [6] incorporated span-wise rows of holes which, by pair-wise combination, generated a so-called anti-kidney-vortex. Na et al. [7] made the surface just upstream of a row of film-cooling holes into a ramp with a backward-facing step. Nasir et al. [8] investigated the effect of discrete delta-shaped tabs with different orientations on the film cooling performance from a row of cylindrical holes. Ghorab et al. [9,10] studied the hybrid and the louver schemes using a thermochromic liquid crystal technique. The results of the above methods all showed high local and average film cooling effectiveness performances and made significant contributions to cooling enhancements. However, the increased benefits of such methods are about to approach their limits [11]. As next-generation turbines are required to burn alternate fuels, their operating temperatures are expected to increase [12]. Furthermore, cooling streams cannot be supplied without limits. Therefore, the developments of advanced, high efficiency cooling methods have become one of the main supporting technologies for high-performance aircraft engines and gas turbines.

Looking further into the mechanism of convective heat transfer, Guo et al. [13] introduced a novel concept of heat transfer enhancement through merging the energy equations of heat conduction and convection. It can be concluded from this concept that there are several ways to decrease the overall strength of convective heat transfer over the thermal boundary layer. One way is to reduce the value of the integral of the internal heat source term (heat sink) over the thermal boundary layer.

Based on the theory of heat transfer enhancement, a novel film cooling method using chemical heat sink is proposed. First, a cooling stream  $\text{NH}_3$  is ejected to the blades' exterior surfaces through discrete holes and is heated by the hot mainstream. At the same time, an endothermic reaction takes place inside the protective film boundary layer. The heat absorbed in the reaction is equivalent to the internal heat source term (heat sink) added to the energy equation for convective heat transfer. According to the theory of heat transfer enhancement, the overall strength of convective heat transfer is decreased and film effectiveness is improved.

In the present study, a novel film cooling method using a chemical reaction with  $\text{NH}_3$  as the cooling stream is simulated numerically on a flat plate with a single cylindrical hole. The effects of the chemical heat sink on film cooling effectiveness are investigated and the conventional film cooling method is also simulated for comparison.

## 1 Physical model

### 1.1 Geometry for the simulation

Figure 1 shows a diagram of the computational domain,

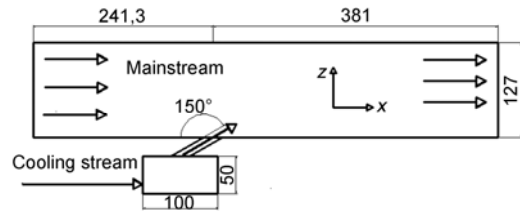


Figure 1 Diagram of the computational domain.

which includes the cooling stream supply channel, the cylindrical cooling hole, and the mainstream channel. The diameter of the cylindrical part of the cooling hole ( $D$ ) was 12.7 mm with an inclination angle of  $30^\circ$  injecting into the mainstream channel, and the ratio of the length of the cooling hole to the diameter of the cooling hole was 4. This paper is presented to confirm the feasibility of the proposed method and it was not considered to adopt a complex geometry for the simulation. Therefore, there was only one hole in the present study and the distance from the center of the film hole to each border was  $1.5D$ . The sizes of the mainstream channel were 622.3 mm in length, 38.1 mm in width and 127 mm in height, and the sizes of the cooling tank were 100 mm in length, 38.1 mm in width and 50 mm in height.

### 1.2 Boundary conditions

The properties of reactant, products and the mainstream were the same as those of an ideal gas. The normal speed of the mainstream was set at 20 m/s. According to the literature [14], under conditions of ordinary pressure and the absence of catalyst conditions, the resolution ratio of  $\text{NH}_3$  at 1000 K is 1%. Therefore, for simulations of the film cooling effect, the temperature of the mainstream was set at 1400 K, and the temperature of the cooling stream was set at 700 K. In addition, the turbulence intensity at the inlet boundary of the mainstream was 2%. The same turbulence intensity was set at the inlet boundary of the cooling stream. The velocity of the cooling stream can be determined from the blowing ratio [15], which is defined as

$$M = \frac{\rho_c U_c}{\rho_g U_g}, \quad (1)$$

where  $\rho$  and  $U$  are the fluid density and velocity, respectively, and the subscripts  $g$  and  $c$  represent the mainstream and the cooling streams, respectively.

In the simulations, adiabatic and no-slip boundary conditions were used for the walls. In addition, periodic conditions at the side-walls of the main channel were specified. The pressure boundary condition was specified at the exit of the mainstream flow channel. The wall-function method was taken in the near wall region and the standard k- $\epsilon$  model was used. The equations were discretized by adopting the second order high-resolution method. The convergence cri-

terion of the solutions was that the relative residual of the physical quantities should be less than  $10^{-5}$ .

## 2 Grids dependency analysis

A preliminary grid dependency test for the geometry was carried out. Three types of node number were tested to find the optimal node number for the geometry shown in Figure 2. From the figure, it can be seen that the film effectiveness of the three types of node number were almost the same, so differences were neglected. Therefore, node number 787200 was selected. The main channel in this study comprised  $200 \times 60 \times 55$  nodes ( $x$ ,  $y$ , and  $z$  directions), and  $80 \times 60 \times 24$  nodes and  $30 \times 20 \times 30$  nodes were used for the cooling tack and round cooling hole, respectively.

## 3 Results and discussion

The objective of this study was to understand the usefulness of the chemical heat sink of the  $\text{NH}_3$  cooling stream in improving film cooling adiabatic effectiveness. All cases simulated are summarized in Table 1.

The computational results were presented and compared by introducing the non-dimensional parameter-local adiabatic film cooling effectiveness [16], defined as

$$\eta = \frac{T_g - T_w}{T_g - T_c}, \quad (2)$$

in which,  $T_g$  is the (constant) mainstream gas temperature, and  $T_c$  is the cooling stream temperature, which typically equals the coolant exit bulk temperature at the injection

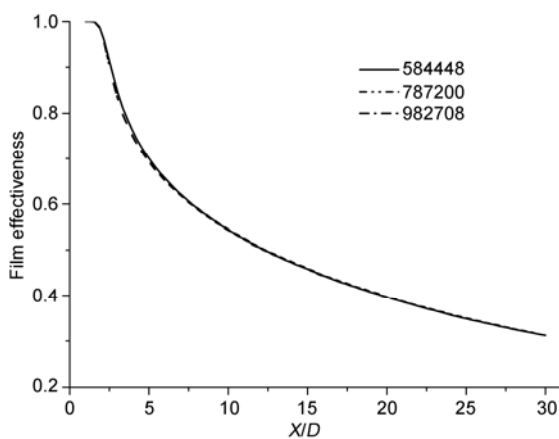


Figure 2 The grid dependency test.

Table 1 Simulation cases

| Case | Method       | Reaction formulas                                   | Reaction heat |
|------|--------------|---|---------------|
| 1    | Conventional | None  | None          |
| 2    | Present      | $2\text{NH}_3 \rightarrow \text{N}_2 + 3\text{H}_2$ | 46.2 kJ/mol   |

point into the mainstream, and  $T_w$  is the adiabatic wall temperature.

### 3.1 Validation

The span-averaged film effectiveness of the cylindrical film hole for Case 1 can be compared with previously published data to validate the current CFD model. The cylindrical geometry was selected since it is the most commonly used baseline geometry in previous studies. The results in Figure 3 show an agreement of more than 90% of the span-averaged film effectiveness with published data by Wayne et al. [17], and Cuong et al. [18]. However, there are some differences between the results obtained in the current study and published data by Dhungel et al. [4]. These discrepancies are expected to result from the high temperature used in the present study. In general, the present numerical results agreed closely with the data reported in the literatures, which demonstrates that the model used in the present study was reliable.

### 3.2 Contours of film effectiveness on the bottom surface

Detailed film cooling effectiveness distributions for the conventional and novel methods are presented in Figure 4. From the figure, it can be clearly seen that Case 2 displays not only a much higher film effectiveness but also a broader jet area than Case 1 at various blowing ratios. This superior performance may be attributed to the chemical heat sink caused by the endothermic reaction of the  $\text{NH}_3$  cooling stream. As a result of the chemical heat sink, the convective heat transfer is weakened between the mainstream and the bottom surface, and the film effectiveness is improved. Because of the decomposition reaction of the  $\text{NH}_3$  cooling stream, the pressure in the film layer is increased, this leads to the expansion of the film along the lateral direction, so Case 2 has a broader jet area downstream of the film hole.

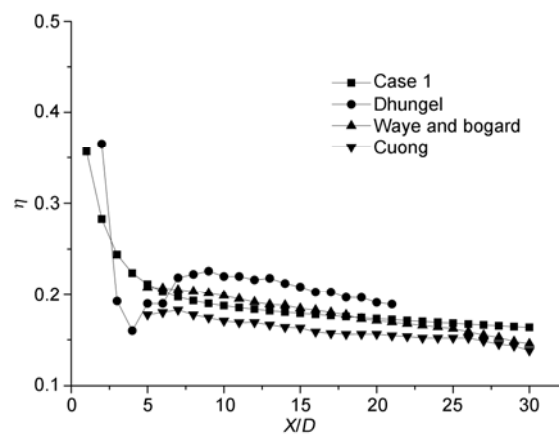
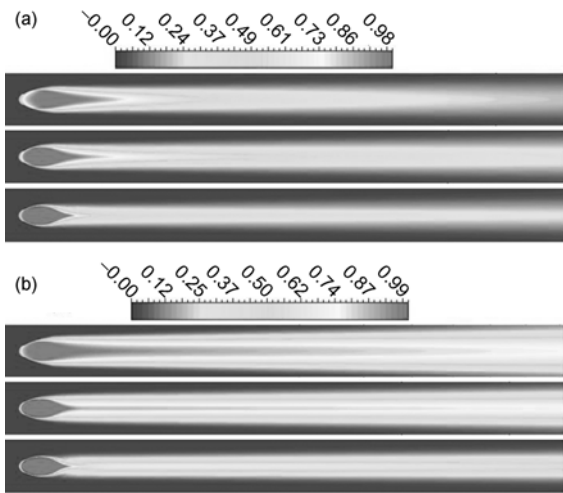


Figure 3 Comparison of span-averaged film effectiveness with reported literature values.



**Figure 4** Film effectiveness on the bottom surface at  $M = 0.5, 1.0,$  and  $1.5.$  (a) Case 1; (b) Case 2.

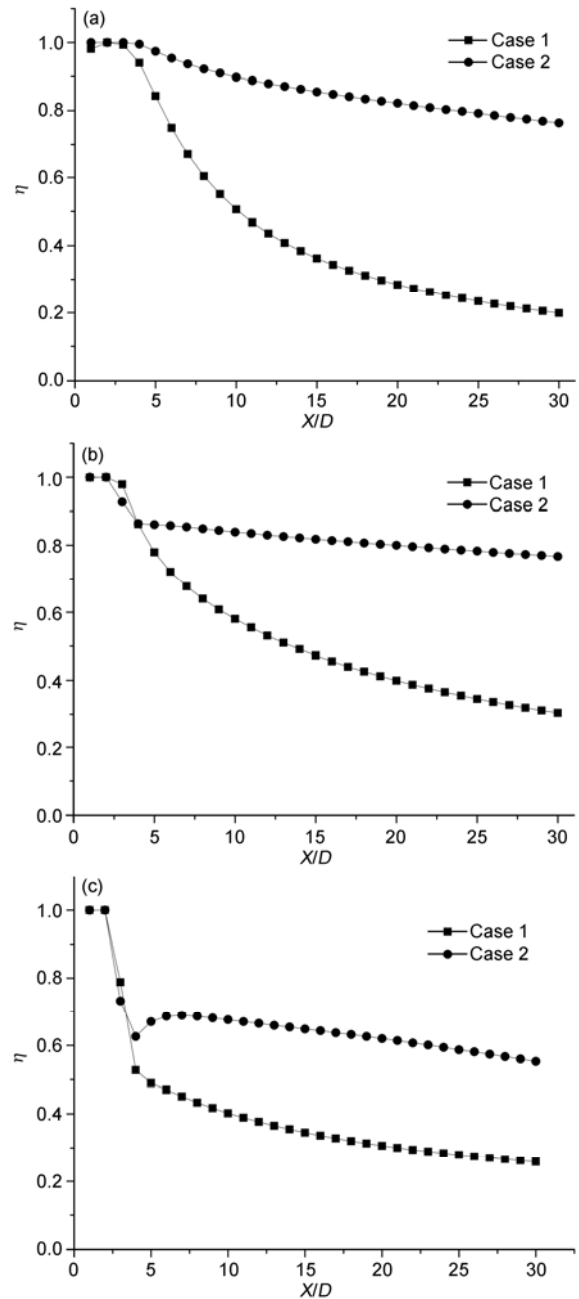
At the same time, the increase in material quality could improve the static pressure of the film layer and play the role of rejection and rebound of the mainstream, which can also enhance film effectiveness.

### 3.3 Distributions of film effectiveness on the centerline

Figure 5 shows a plot of centerline film effectiveness values downstream of the film hole for two cases.  $X/D$  is defined as the ratio of downstream distance from the center of the film hole to the diameter of the film hole. From the figure, it can be seen that there is little difference in film effectiveness between the two cases in the region  $X/D < 4$ . This is because the conventional method has a very high film effectiveness in this region and therefore the effect of the chemical heat sink on the improvements in film effectiveness for Case 2 is not marked. In the region  $X/D > 4$ , at  $M = 0.5$  and  $1.0$ , film effectiveness decreases gradually for Case 2, because of the presence of the chemical heat sink. This is in contrast to the behavior in Case 1 at various blowing ratios, where film effectiveness is markedly decreased downstream of the film hole. The film effectiveness is improved by 283.92% and 152.3% at the location  $X/D = 30$ . At  $M = 1.5$ , because of the high momentum of the cooling stream, significant amounts of  $\text{NH}_3$  have little time to take part in the chemical reaction. Therefore, the film cooling effectiveness is markedly decreased downstream but increased by about 0.3 over a wide range of stream-wise directions compared with the conventional case.

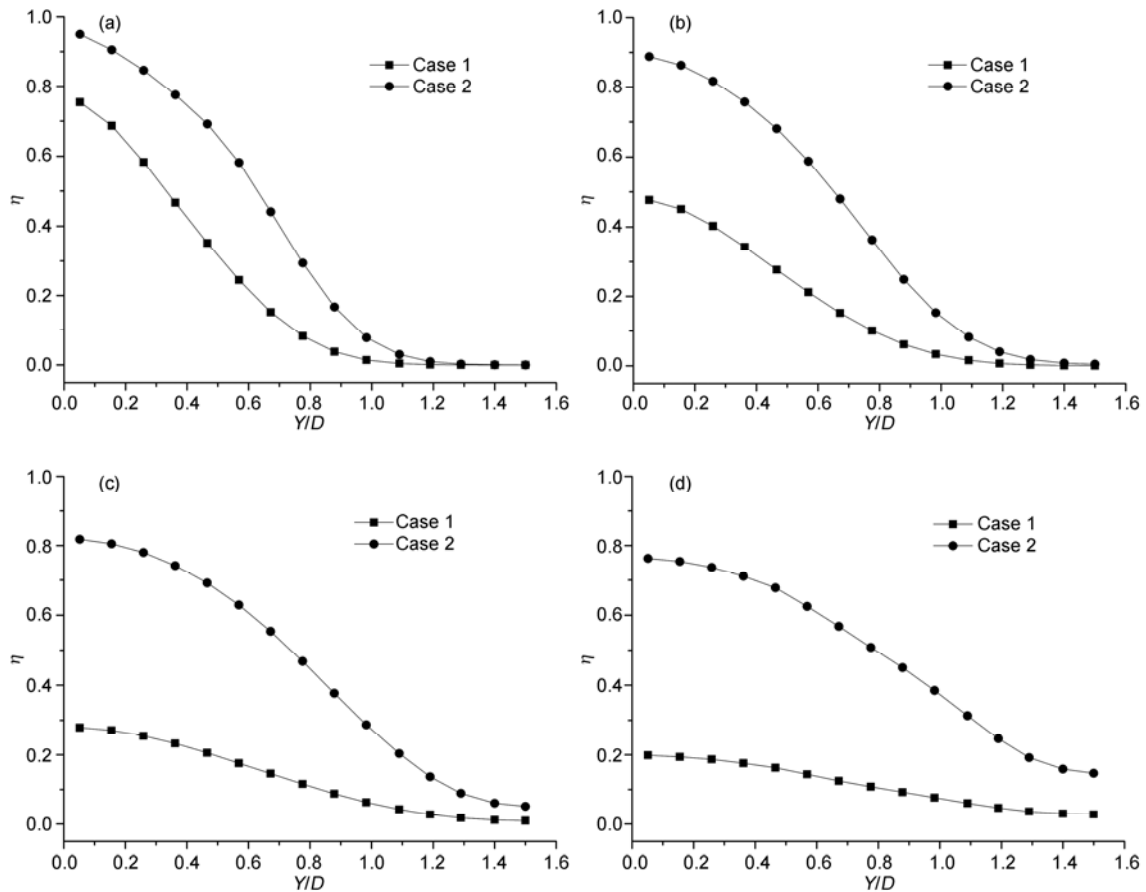
### 3.4 Distributions of span-wise film effectiveness

Figure 6 shows the comparison of span-wise film effectiveness for two cases when the blowing ratio is 0.5. From the figure, it can be seen that Case 2 shows a higher film effec-



**Figure 5** Centerline film effectiveness at different blowing ratios. (a)  $M = 0.5;$  (b)  $M = 1.0;$  (c)  $M = 1.5.$

tiveness in the span-wise direction. The differences between the two cases in film effectiveness increased with  $X/D$ . It also can be seen that there were some regions where the cooling stream could not reach for Case 1, so film cooling did not work in these regions. For Case 2, between the location of  $X/D = 10$  and  $20$  downstream of the film hole, there was a location where the cooling stream began to cover the whole bottom surface, therefore, improving the film effectiveness close to the borders, compared with Case 1. There is no doubt that the improvement was the effect of the chemical heat sink caused by the  $\text{NH}_3$  cooling stream.



**Figure 6** Span-wise film effectiveness at different locations. (a)  $X/D = 5$ ; (b)  $X/D = 10$ ; (c)  $X/D = 20$ ; (d)  $X/D = 30$ .

### 3.5 Span-averaged film effectiveness

Figure 7 shows the comparison of span-averaged film effectiveness for the conventional and the novel methods on the flat plate. When the blowing ratio was above 1.0, in the region  $0 < X/D < 2.5$ , there was not little differences in span-averaged film effectiveness between the two cases. However, in the region  $X/D > 2.5$ , larger amounts of  $\text{NH}_3$  absorb heat and join the reaction downstream of the film hole, so the span-averaged film effectiveness for Case 2 improved gradually with  $X/D$ . This is in contrast to the behavior in Case 1 at various blowing ratios, where effectiveness slowly decreased downstream of the film hole. When the blowing ratio was 0.5, the momentum of the  $\text{NH}_3$  cooling stream was so low that there was enough time to take part in the chemical reaction. Therefore, the span-averaged film effectiveness for Case 2 is always higher than that for Case 1. From the figure, it can be seen that the differences between the two cases were reduced as blowing ratio increased. The span-averaged film effectiveness was improved by 333.78%, 131.19%, and 73.78% at the location  $X/D = 30$  for  $M = 0.5$ , 1.0, and 1.5, respectively.

### 3.6 Film effectiveness for Case 2

Figure 8 shows the centerline film effectiveness and

span-averaged film effectiveness on the bottom surface for Case 2.  $Y/D$  is defined as the ratio of lateral distance measured from the axis of the film hole to the diameter of the film hole. From the figure, it can be concluded that regardless of the centerline film effectiveness or the span-averaged film effectiveness, both decreased with increasing blowing ratio and Case 2 presented the best performance at  $M = 0.5$ . A reason for this can be found in Figures 9 and 10. Figure 9 shows the mass fraction of  $\text{NH}_3$  at  $X/D = 3$  and Figure 10 shows the mass fraction of  $\text{NH}_3$  at  $Y/D = 0$ . The fluid dynamic behavior of the  $\text{NH}_3$  cooling stream is rather complex, which differs from that of the cooling air in the conventional method. On one hand, the velocity of  $\text{NH}_3$  is higher than that of cooling air at the same blowing ratio, because of it having a different density. On the other hand, an endothermic reaction takes place in the protective film layer. As shown in Figure 9, the well-known counter-rotating vortex pair causes the cooling stream to separate from the bottom surface at  $M = 1.0$  and  $M = 1.5$ . This vorticity significantly reduces the cooling effectiveness. Figure 10(b) and (c) also demonstrates that the cooling stream is more severely separated from the bottom surface with increasing blowing ratio and  $X/D$ . However, when the blowing ratio was 0.5, the velocity of the cooling stream was not sufficient to produce

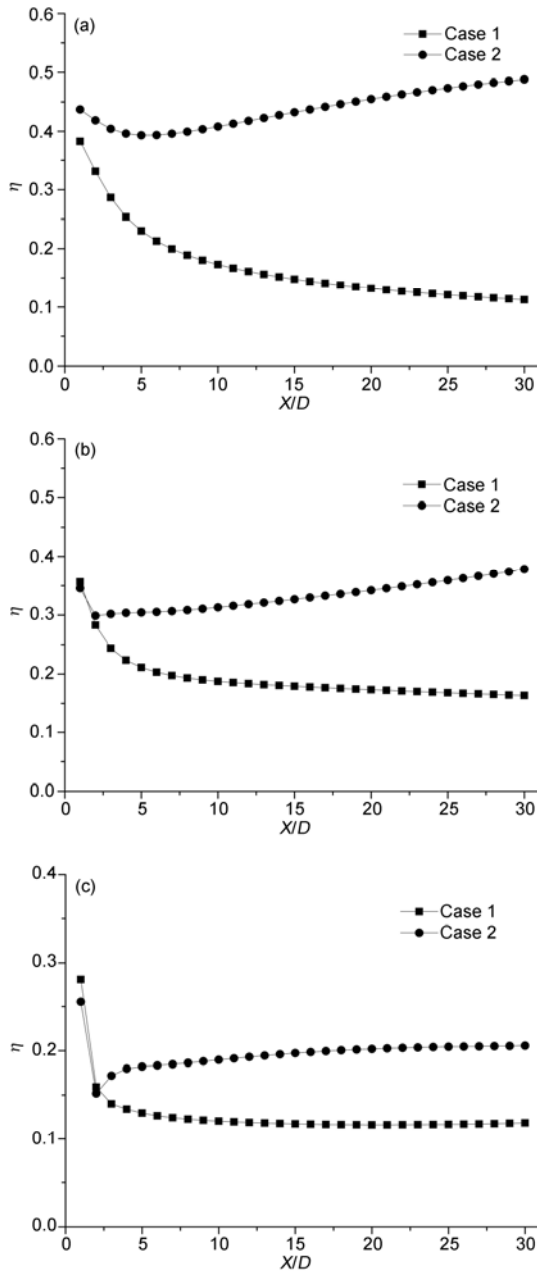


Figure 7 Span-averaged film effectiveness at different blowing ratios. (a)  $M = 0.5$ ; (b)  $M = 1.0$ ; (c)  $M = 1.5$ .

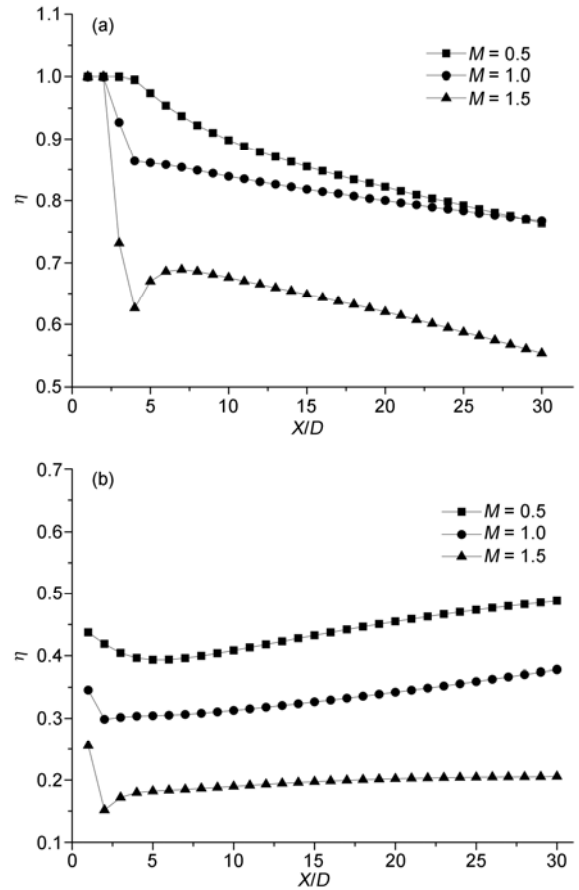


Figure 8 Centerline and span-averaged film effectiveness for Case 2.

the counter-rotating-vortex pair, and the cooling stream remained attaching to the bottom surface, as shown in Figures 9 and 10(a).

### 4 Conclusions

In the present study, based on the theory of heat transfer enhancement, a novel film cooling method using a chemical heat sink caused by the decomposition reaction of an  $\text{NH}_3$  cooling stream was proposed. This novel method was

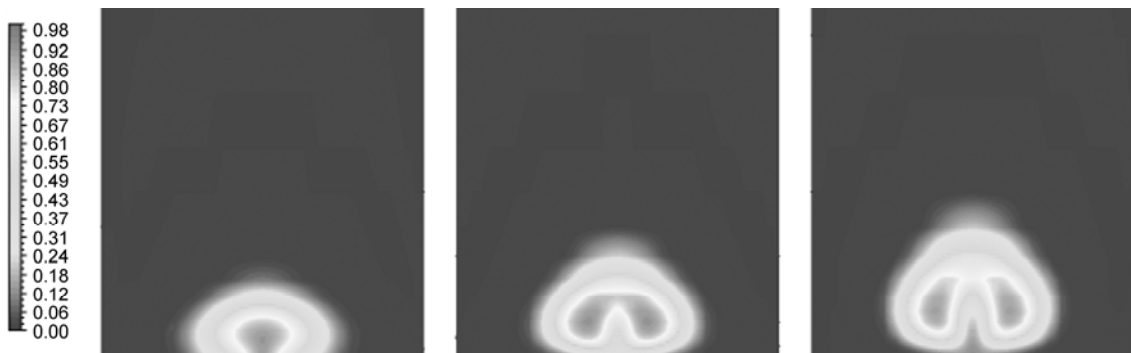


Figure 9 Mass fraction of  $\text{NH}_3$  on the  $Y-Z$  plane at  $M = 0.5, 1.0, \text{ and } 1.5$ .



**Figure 10** Mass fraction of  $\text{NH}_3$  on the X-Z plane at different blowing ratios. (a)  $M = 0.5$ ; (b)  $M = 1.0$ ; (c)  $M = 1.5$ .

simulated on a flat plate with a cylindrical hole. The results show that this novel method has better performance at a low blowing ratio, because the fluid dynamic behavior of the  $\text{NH}_3$  cooling stream is somewhat complicated, and the velocity of the cooling stream is not sufficient to produce the counter-rotating vortex pair. Therefore, the cooling stream remains attached to the bottom surface. The results also show that film effectiveness is enhanced with increasing  $X/D$  at various blowing ratios, which is in contrast to the behavior in the conventional method, where film effectiveness is markedly decreased downstream of the film hole. Compared with the conventional film cooling method, this novel approach can even enhance the film effectiveness of the regions close to the borders. All of the improvements described above can be attributed to the effect of the chemical heat sink caused by the decomposition reaction of the  $\text{NH}_3$  cooling stream.

*This work was supported by the National Natural Science Foundation of China (50976118) and the National Basic Research Program of China (2010CB227302).*

- 1 Kercher D M. A film-cooling CFD bibliography: 1971-1996. *Int J Rotating Machinery*, 1998, 4: 61-72
- 2 Bunker R S. A review of shaped hole turbine film-cooling technology. *J Heat Transfer*, 2005, 127: 441-454
- 3 Heidmann J D, Ekkad S V. A novel anti-vortex turbine film-cooling hole concept. *J Turbomach*, 2008, 130: 031020
- 4 Dhungel A, Lu Y P, Phillips W, et al. Film cooling from a row of holes supplemented with anti vortex holes. *J Turbomach*, 2009, 131: 021007
- 5 Heidmann J D. A numerical study of anti-vortex film-cooling designs at high blowing ratio. Technical Report, Gas Turbine Technical Congress, National Aeronautics and Space Administration, 2008
- 6 Gräf L, Kleiser L. Large-eddy simulation of double-row compound-angle film cooling: Setup and validation. *Comput Fluids*, 2011, 43: 58-67
- 7 Na S, Shih T I. Increasing adiabatic film-cooling effectiveness by using an upstream ramp. *J Heat Transfer*, 2007, 129: 464-471
- 8 Nasir H, Acharya S, Ekkas S V. Improved film cooling from cylindrical angled holes with triangular tabs: Effect of tab orientations. *Int J Heat Fluid Flow*, 2003, 24: 657-668
- 9 Ghorab M G. Film cooling effectiveness and net heat flux reduction of advanced cooling schemes using thermochromic liquid crystal. *Appl Therm Eng*, 2011, 31: 77-92
- 10 Ghorab M G, Hassan I G. An experimental investigation of a new hybrid film cooling scheme. *Int J Heat Mass Transfer*, 2010, 53: 4994-5007
- 11 Burdet A, Abhari R S. Influence of near hole pressure fluctuation on the thermal protection of a film-cooled flat plate. *J Heat Transfer*, 2009, 131: 022202
- 12 Li X, Wang T. Simulation of film cooling enhancement with mist injection. *J Heat Transfer*, 2006, 128: 509-520
- 13 Guo Z Y, Li D Y, Wang B X. A novel concept for convective heat transfer enhancement. *Int J Heat Mass Transfer*, 1998, 41: 2221-2225
- 14 Chang L. Research of supported Ni-based catalysts for ammonia decomposition (in Chinese). Master Dissertation. Tianjin: Tianjin University, 2008
- 15 Lee K D, Kim K Y. Shape optimization of a fan-shaped hole to enhance film-cooling effectiveness. *Int J Heat Mass Transfer*, 2010, 53: 2996-3005

- 16 Li G C, Zhu H R, Fan H M. Influences of hole shape on film cooling characteristics with CO<sub>2</sub> injection. *Chin J Aeronaut*, 2008, 21: 393–401
- 17 Wayne S K, Bogard D G. High resolution film cooling effectiveness measurements of axial holes embedded in a transverse trench with various trench configurations. *J Turbomach*, 2007, 129: 294–303
- 18 Nguyen C Q, Johnson P L, Bernier B C, et al. Comparison of film effectiveness and cooling uniformity of conical and cylindrical-shaped film hole with coolant-exit temperature correction. *J Thermal Sci Eng Appl*, 2011, 3: 031011

**Open Access** This article is distributed under the terms of the Creative Commons Attribution License which permits any use, distribution, and reproduction in any medium, provided the original author(s) and source are credited.